

QCD instantons at hadron colliders

Valya Khoze

IPPP Durham

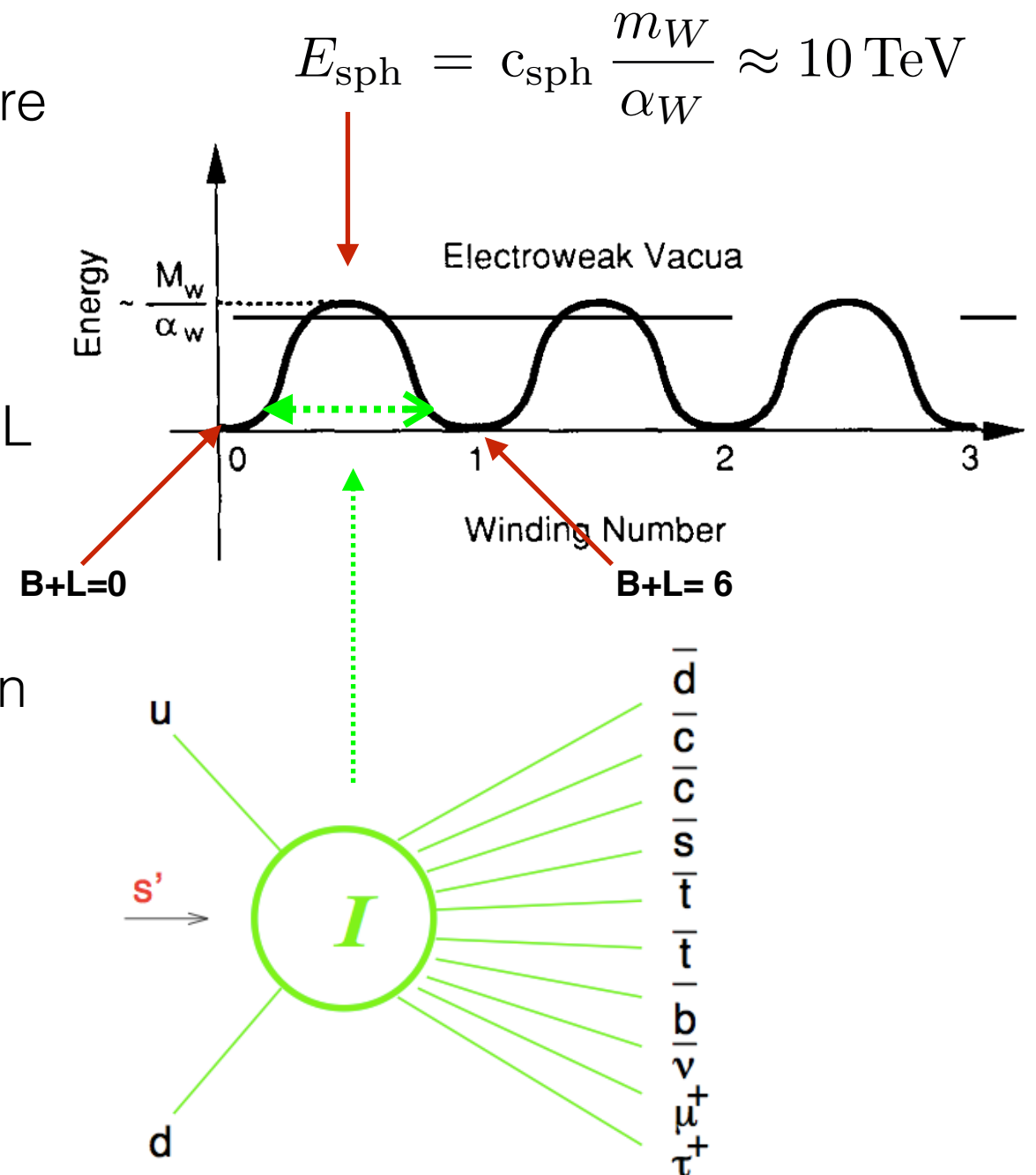
with Frank Krauss & Matthias Schott 1911.09726 : JHEP

and Dan Milne & Michael Spannowsky 2010.02287 : PRD

& with Valery A Khoze, Dan Milne and Misha Ryskin
2104.01861 : PRD, 2111.02159

Warm-up: Electro-Weak Instantons

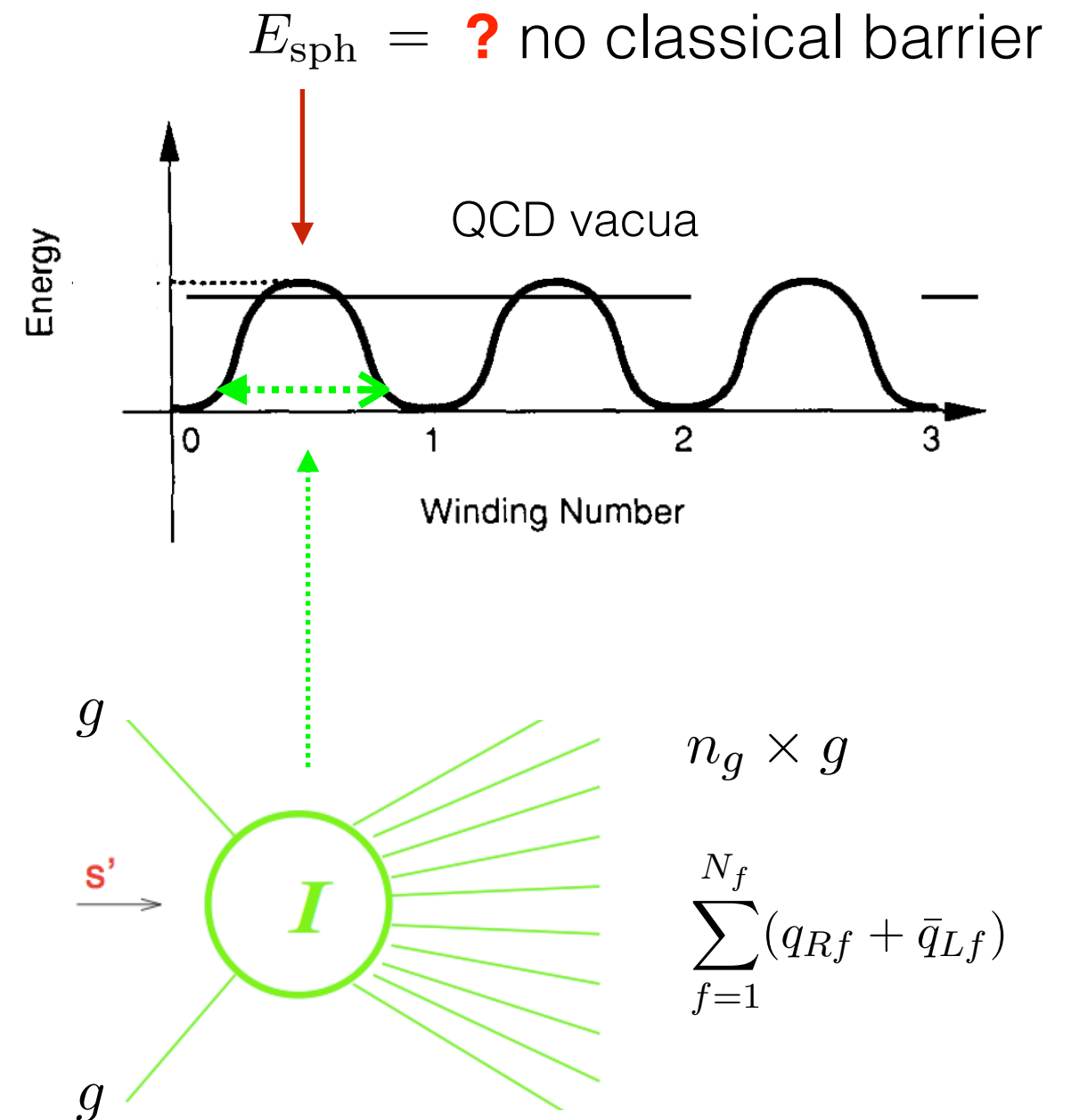
- Yang-Mills vacuum has a nontrivial structure
- The saddle-point at the top of the barrier is the *sphaleron*. New EW scale ~ 10 TeV
- Transitions between the vacua change B+L (result of the ABJ anomaly):
 $\Delta(B+L) = 3 \times (1+1)$; $\Delta(B-L) = 0$
- *Instantons* are tunnelling solutions between the vacua. They mediate B+L violation
- $3 \times (1 \text{ lepton} + 3 \text{ quarks}) = 12$ fermions
 12 left-handed fermion doublets are involved
- There are EW processes which are not described by perturbation theory!



$$q + q \rightarrow 7\bar{q} + 3\bar{l} + n_W W + n_Z Z + n_h H$$

QCD Instantons

- Yang-Mills vacuum has a nontrivial structure
- *Instantons* are tunnelling solutions between the vacua.
- At the classical level there is no barrier in QCD. The *sphaleron* is a quantum effect
- Transitions between the vacua change chirality (result of the ABJ anomaly).
- All light quark-anti-quark pairs must participate in the reaction
- Not described by perturbation theory.



$$g + g \rightarrow n_g \times g + \sum_{f=1}^{N_f} (q_{Rf} + \bar{q}_{Lf})$$

QCD Instantons

Instanton-induced processes with 2 gluons in the initial state:

$$g + g \rightarrow n_g \times g + \sum_{f=1}^{N_f} (q_{Rf} + \bar{q}_{Lf})$$

\uparrow
 \vdots
 arbitrary
 (tends to be large $\sim 1/\alpha_s$)

All light flavours of quark-antiquark
 pairs must be present. Light \Rightarrow
 $m_f \leq 1/\rho$
 \uparrow
 \vdots
 instanton size

Can also have quark-initiated processes e.g. :

$$u_L + \bar{u}_R \rightarrow n_g \times g + \sum_{f=1}^{N_f-1} (q_{Rf} + \bar{q}_{Lf}) ,$$

$$u_L + d_L \rightarrow n_g \times g + u_R + d_R + \sum_{f=1}^{N_f-2} (q_{Rf} + \bar{q}_{Lf})$$

$$g + g \rightarrow n_g \times g + \sum_{f=1}^{N_f} (q_{Rf} + \bar{q}_{Lf})$$

The amplitude takes the form of an integral over instanton collective coordinates.
The classical result (leading order in the instanton perturbation theory) is simply:

semiclassical suppression
(’t Hooft) factor by the instanton action

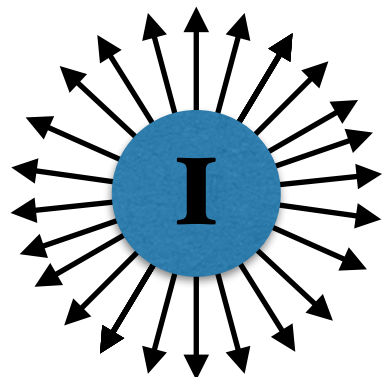
$$S_I = \frac{8\pi^2}{g^2} = \frac{2\pi}{\alpha_s(\mu_r)}$$

⋮
↓

$$\mathcal{A}_{2 \rightarrow n_g + 2N_f} \sim \int d^4x_0 d\rho D(\rho) e^{-S_I} \left[\prod_{i=1}^{n_g+2} A_{\text{LSZ}}^{a_i \text{ inst}}(p_i, \lambda_i) \right] \left[\prod_{j=1}^{2N_f} \psi_{\text{LSZ}}^{(0)}(p_j, \lambda_j) \right]$$

↗ ↗
⋮ ⋮

- the integrand: a product of bosonic and fermionic components of the instanton field configurations
- the factorised structure implies that emission of individual particles in the final state is uncorrelated and mutually independent.

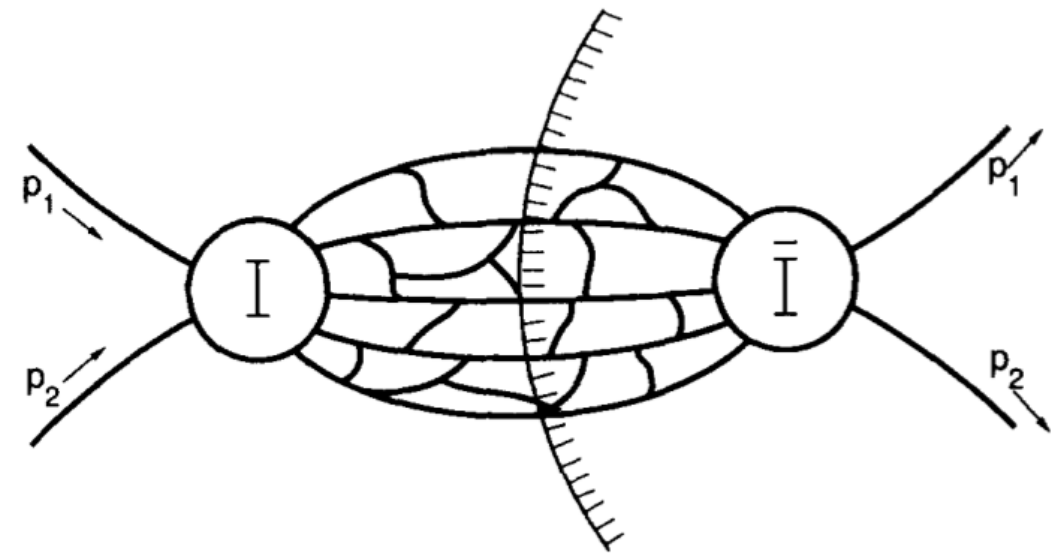
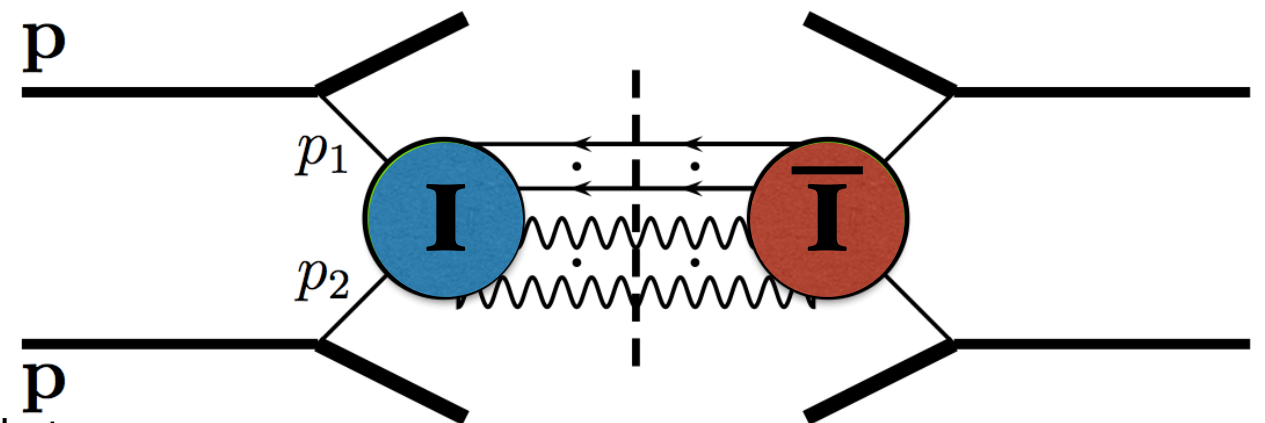


[this is correct at the LO in instanton pert. theory approximation]
LO Instanton vertex

The Optical Theorem approach: to include final state interactions

$$\hat{\sigma}_{\text{tot}}^{\text{inst}} = \frac{1}{E^2} \text{Im} \mathcal{A}_4^{I\bar{I}}(p_1, p_2, -p_1, -p_2)$$

- Cross-section is obtained by |squaring| the instanton amplitude.
- Final states have been instrumental in combatting the exp. suppression.
- Now also the interactions between the final states (and the improvement on the point-like I-vertex) are taken into account.
- Use the Optical Theorem to compute *Im* part of the 2->2 amplitude in around the Instanton-Anti-instanton configuration.
- Varying the energy E changes the dominant value of I-Ibar separation R. At R=0 instanton and anti-instanton mutually annihilate.
- The suppression of the EW instanton cross-section is gradually reduced at lower R(E).



VVK & Ringwald 1991

The Optical Theorem approach: to include final state interactions

- Instanton — anti-instanton valley configuration has $Q=0$; it interpolates between infinitely separated instanton—anti-instanton and the perturbative vacuum at $R=0$

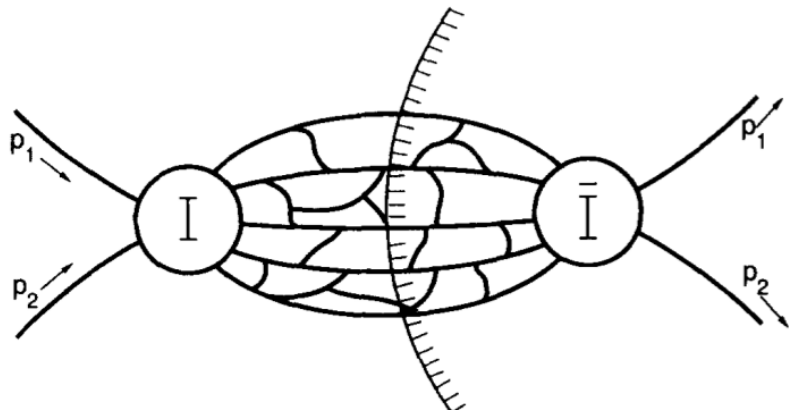
$$\sigma_{\text{tot}}^{(\text{cl}) \text{ inst}} \simeq \frac{1}{s} \text{Im} \int_0^\infty d\rho \int_0^\infty d\bar{\rho} \int d^4 R \int d\Omega D(\rho) D(\bar{\rho}) e^{-S_{I\bar{I}}} \mathcal{K}_{\text{ferm}} \times$$

$$A_{LSZ}^{\text{inst}}(p_1) A_{LSZ}^{\text{inst}}(p_2) A_{LSZ}^{\text{inst}}(-p_1) A_{LSZ}^{\text{inst}}(-p_2),$$

(anti)-instanton sizes (anti)-instanton separation

$S_{I\bar{I}}(\rho, \bar{\rho}, R) = \frac{4\pi}{\alpha_s(\mu_r)} \hat{S}$

instanton-anti-instanton action
(see next slide)



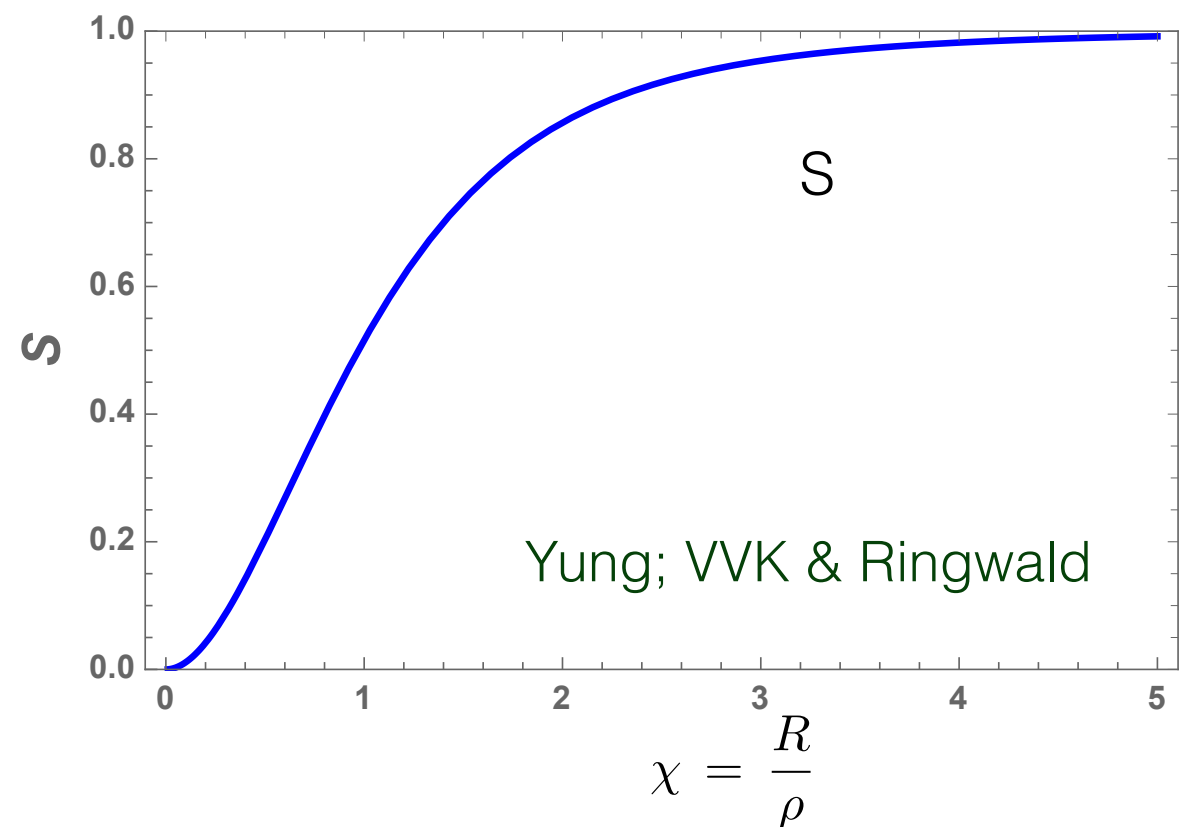
- Exponential suppression is gradually reduced at lower R (Energy-dependent)
- no radiative corrections from hard initial states included in this approximation

$$\begin{aligned}
\sigma_{\text{tot}}^{(\text{cl}) \text{ inst}} &= \frac{1}{s} \text{Im} \mathcal{A}_4^{I\bar{I}}(p_1, p_2, -p_1, -p_2) \\
&\simeq \frac{1}{s} \text{Im} \int_0^\infty d\rho \int_0^\infty d\bar{\rho} \int d^4 R \int d\Omega D(\rho) D(\bar{\rho}) e^{-S_{I\bar{I}}} \mathcal{K}_{\text{ferm}} \times \\
&\quad A_{LSZ}^{\text{inst}}(p_1) A_{LSZ}^{\text{inst}}(p_2) A_{LSZ}^{\text{inst}}(-p_1) A_{LSZ}^{\text{inst}}(-p_2),
\end{aligned}$$



$$\mathcal{S}(\chi) \simeq 1 - 6/\chi^4 + 24/\chi^6 + \dots \quad \chi = \frac{R}{\rho}$$

$$S_{I\bar{I}}(\rho, \bar{\rho}, R) = \frac{4\pi}{\alpha_s(\mu_r)} \mathcal{S}$$



- Exponential suppression is gradually reduced at lower and lower $\chi = \frac{R}{\rho}$
- no radiative corrections from hard initial states included in this approximation

$$D(\rho, \mu_r) = \kappa \frac{1}{\rho^5} \left(\frac{2\pi}{\alpha_s(\mu_r)} \right)^6 (\rho \mu_r)^{b_0}$$

$$\begin{aligned} \sigma_{\text{tot}}^{(\text{cl}) \text{ inst}} &= \frac{1}{s} \text{Im} \mathcal{A}_4^{I\bar{I}}(p_1, p_2, -p_1, -p_2) \\ &\simeq \frac{1}{s} \text{Im} \int_0^\infty d\rho \int_0^\infty d\bar{\rho} \int d^4 R \int d\Omega D(\rho) D(\bar{\rho}) e^{-S_{I\bar{I}}} \mathcal{K}_{\text{ferm}} \times \\ &\quad A_{LSZ}^{\text{inst}}(p_1) A_{LSZ}^{\text{inst}}(p_2) \overline{A_{LSZ}^{\text{inst}}(-p_1)} \overline{A_{LSZ}^{\text{inst}}(-p_2)}, \end{aligned}$$

fermion prefactor
from Nf qq-bar pairs

$$A_{LSZ}^{\text{inst}}(p_1) A_{LSZ}^{\text{inst}}(p_2) \overline{A_{LSZ}^{\text{inst}}(-p_1)} \overline{A_{LSZ}^{\text{inst}}(-p_2)} = \frac{1}{36} \left(\frac{2\pi^2}{g} \rho^2 \sqrt{s'} \right)^4 e^{iR \cdot (p_1 + p_2)}$$

$$\exp \left(R_0 \sqrt{s} - \frac{4\pi}{\alpha_s(\mu_r)} \hat{\mathcal{S}}(z) \right)$$

But the instanton size has not been stabilised.
In QCD - **rho** is a **classically flat direction** —
need to **include and re-sum quantum corrections!**

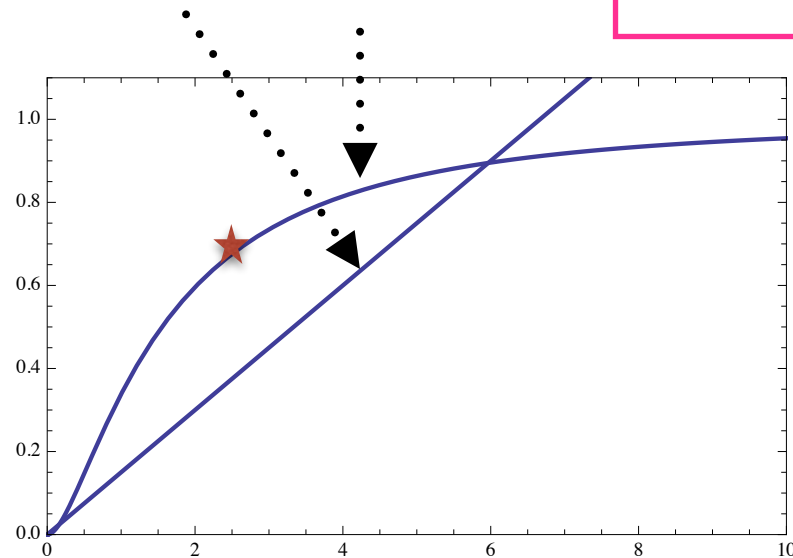
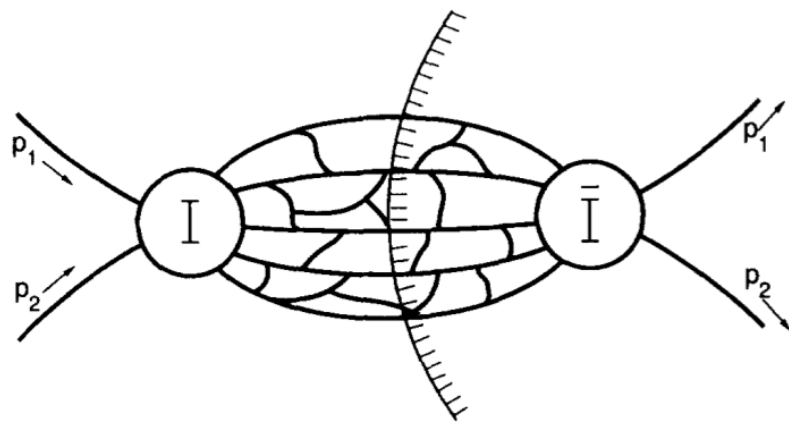
in the EW theory:

$$G_{4\text{Eucl}} \sim \int d^4 R \, d\rho_I d\rho_{\bar{I}} \dots \exp \left[i(p_1 + p_2) \cdot R - S_{I\bar{I}}(z) - \pi^2 v^2 (\rho_I^2 + \rho_{\bar{I}}^2) \right]$$

\nearrow instanton separation \nearrow instanton sizes \nearrow $z \sim \frac{R^2 + \rho_I^2 + \rho_{\bar{I}}^2}{\rho_I \rho_{\bar{I}}}$

\nearrow Higgs vev:
EW theory - **not QCD!**

$$\sigma_{B+L} \sim \text{Im} \int d^4 R \, d\rho_I d\rho_{\bar{I}} \dots \exp \left[ER - S_{I\bar{I}}(R) - \pi^2 v^2 (\rho_I^2 + \rho_{\bar{I}}^2) \right]$$



\nearrow Higgs vev cuts-off
large instantons

- Exponential suppression is gradually reduced with energy [in the EW theory]

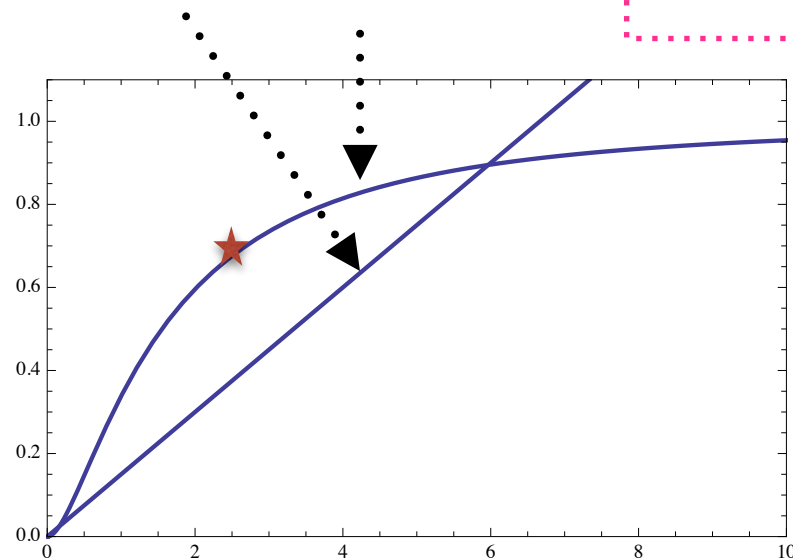
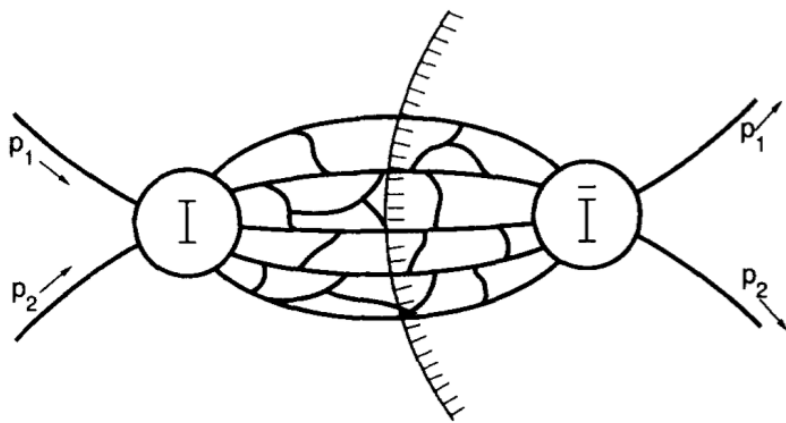
In QCD:

$$G_{4\text{Eucl}} \sim \int d^4 R \, d\rho_I d\rho_{\bar{I}} \dots \exp \left[i(p_1 + p_2) \cdot R - S_{I\bar{I}}(z) \right] \quad \text{- new in QCD}$$

\nearrow instanton separation \nearrow instanton sizes \nearrow $z \sim \frac{R^2 + \rho_I^2 + \rho_{\bar{I}}^2}{\rho_I \rho_{\bar{I}}}$

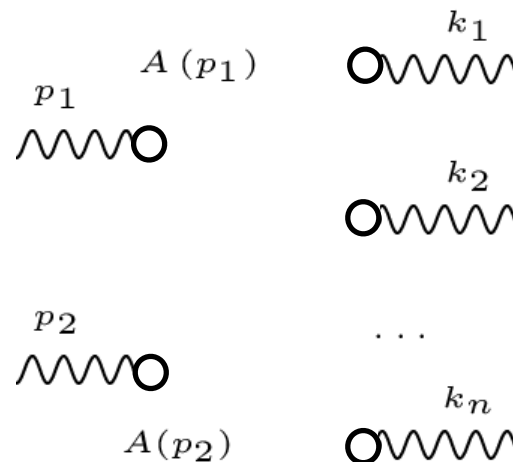
Quantum effects to cut-off
Instanton size integrations

$$\sigma_{B+L} \sim \text{Im} \int d^4 R \, d\rho_I d\rho_{\bar{I}} \dots \exp \left[ER - S_{I\bar{I}}(R) \right] \quad \text{- new in QCD}$$

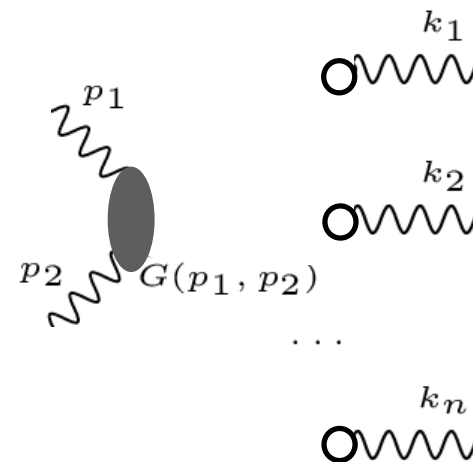


Initial state interactions in the instanton approach

LO instanton process



NLO instanton process



propagator in the instanton background

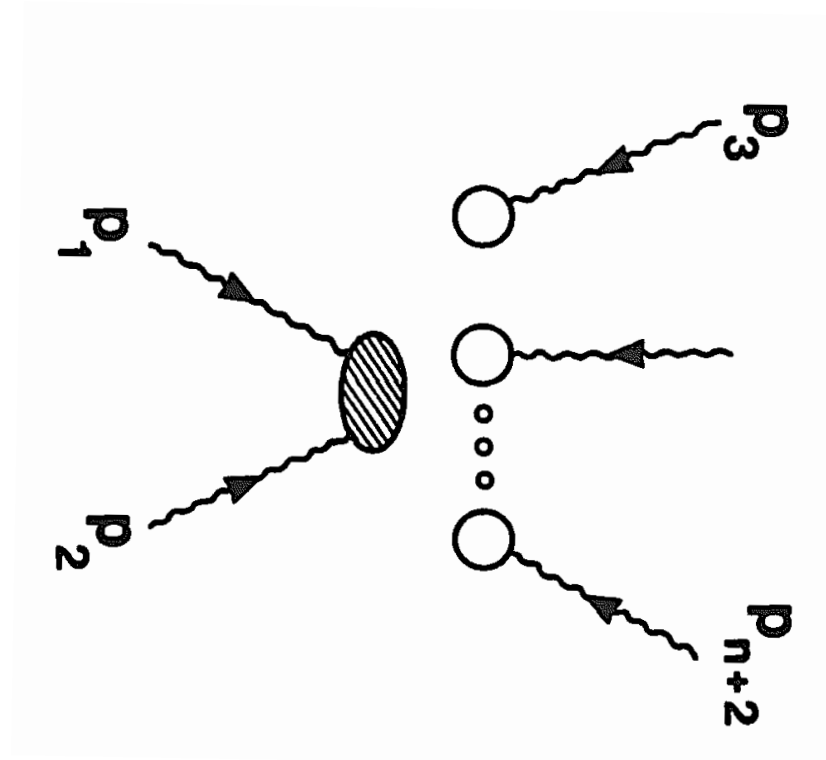
$$G_{\mu\nu}^{ab}(p_1, p_2) \rightarrow -\frac{g^2 \rho^2 s}{64\pi^2} \log(s) A_\mu^a(p_1) A_\nu^b(p_2)$$

$$p_1^2 = 0 = p_2^2, \quad 2p_1 p_2 = s \gg 1/\rho^2$$

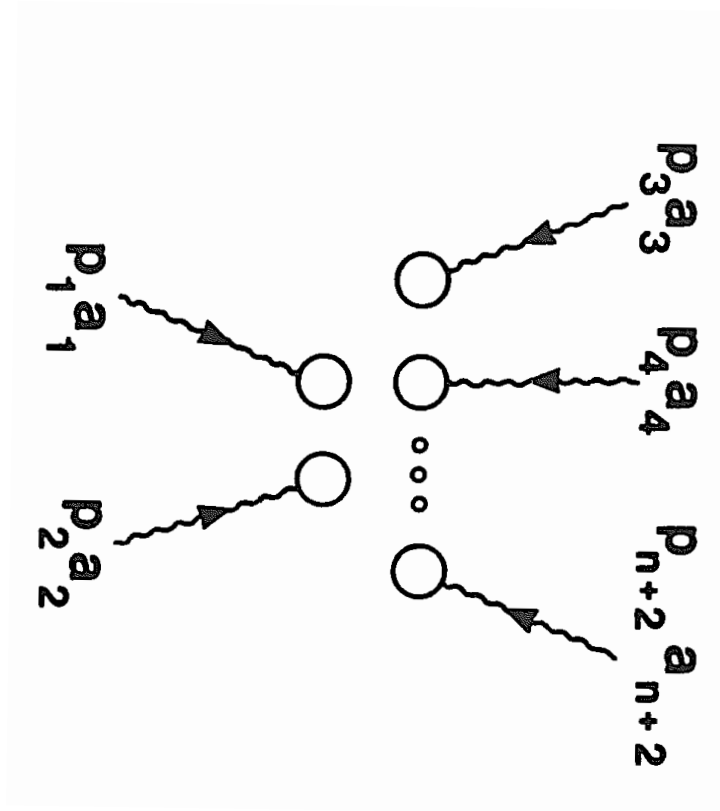
Include now higher order corrections in the high-energy limit:

$$\sum_{r=1}^N \frac{1}{r!} \left(-\frac{g^2 \rho^2 s}{64\pi^2} \log(s) \right)^r A_\mu^a(p_1) A_\nu^b(p_2)$$

Mueller 1991

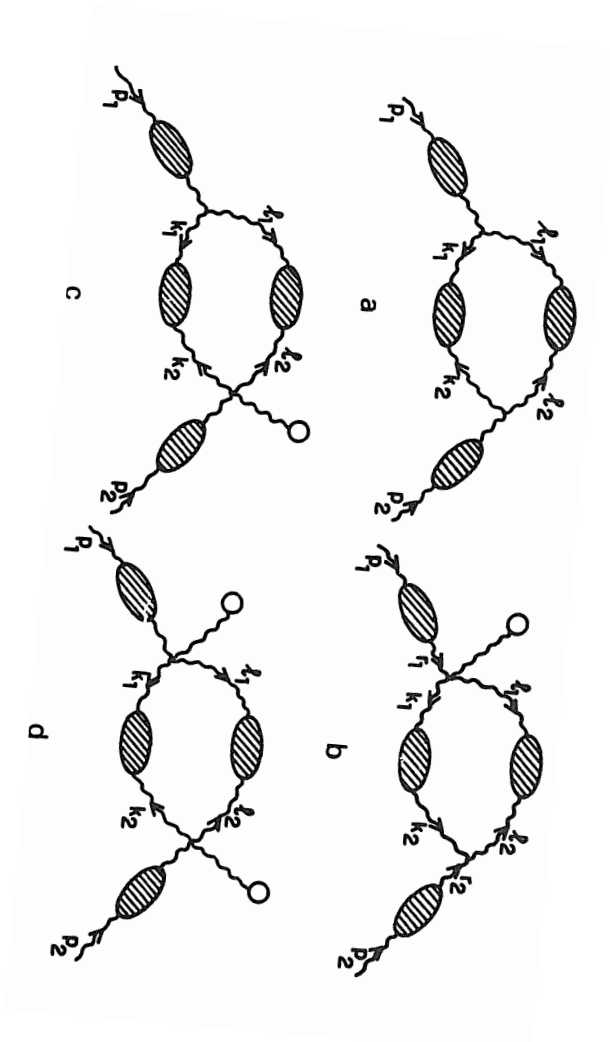
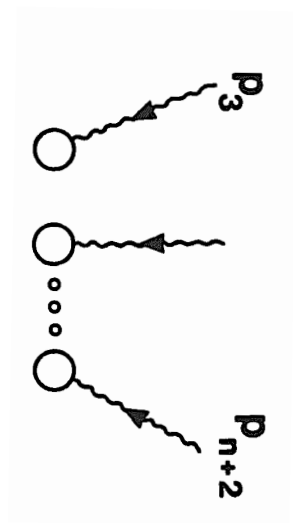


+



+ ...

$$e^{-(\alpha_s(\mu_r)/16\pi) \rho^2 E^2 \log E^2 / \mu_r^2}$$



+

Mueller 1991

Combined effect of initial and final states interactions in QCD

$$\hat{\sigma}_{\text{tot}}^{\text{inst}} \simeq \frac{1}{s'} \text{Im} \frac{\kappa^2 \pi^4}{36 \cdot 4} \int \frac{d\rho}{\rho^5} \int \frac{d\bar{\rho}}{\bar{\rho}^5} \int d^4 R \int d\Omega \left(\frac{2\pi}{\alpha_s(\mu_r)} \right)^{14} (\rho^2 \sqrt{s'})^2 (\bar{\rho}^2 \sqrt{s'})^2 \mathcal{K}_{\text{ferm}} (\rho \mu_r)^{b_0} (\bar{\rho} \mu_r)^{b_0} \exp \left(R_0 \sqrt{s'} - \frac{4\pi}{\alpha_s(\mu_r)} \hat{\mathcal{S}}(z) - \frac{\alpha_s(\mu_r)}{16\pi} (\rho^2 + \bar{\rho}^2) s' \log \left(\frac{s'}{\mu_r^2} \right) \right)$$



Instanton size is cut-off by $\sim \sqrt{s}$
this is what sets the
effective QCD sphaleron scale



Mueller's result for
quantum corrections
due to in-in states
interactions

Basically, in QCD one can never reach the effective sphaleron barrier — it's height grows with the energy.

=> Among other things, no problems with unitarity.

This is the main idea of the approach:

- [1] VVK, Krauss, Schott
- [2] VVK, Milne, Spannowsky

Combined effect of initial and final states interactions in QCD

$$\hat{\sigma}_{\text{tot}}^{\text{inst}} \simeq \frac{1}{s'} \text{Im} \frac{\kappa^2 \pi^4}{36 \cdot 4} \int \frac{d\rho}{\rho^5} \int \frac{d\bar{\rho}}{\bar{\rho}^5} \int d^4 R \int d\Omega \left(\frac{2\pi}{\alpha_s(\mu_r)} \right)^{14} (\rho^2 \sqrt{s'})^2 (\bar{\rho}^2 \sqrt{s'})^2 \mathcal{K}_{\text{ferm}} (\rho \mu_r)^{b_0} (\bar{\rho} \mu_r)^{b_0} \exp \left(R_0 \sqrt{s'} - \frac{4\pi}{\alpha_s(\mu_r)} \hat{\mathcal{S}}(z) - \frac{\alpha_s(\mu_r)}{16\pi} (\rho^2 + \bar{\rho}^2) s' \log \left(\frac{s'}{\mu_r^2} \right) \right)$$

1st Approach: VVK, Krauss, Schott



1. Extermise the holy-grail function in the exponent by finding a saddle-point in variables:

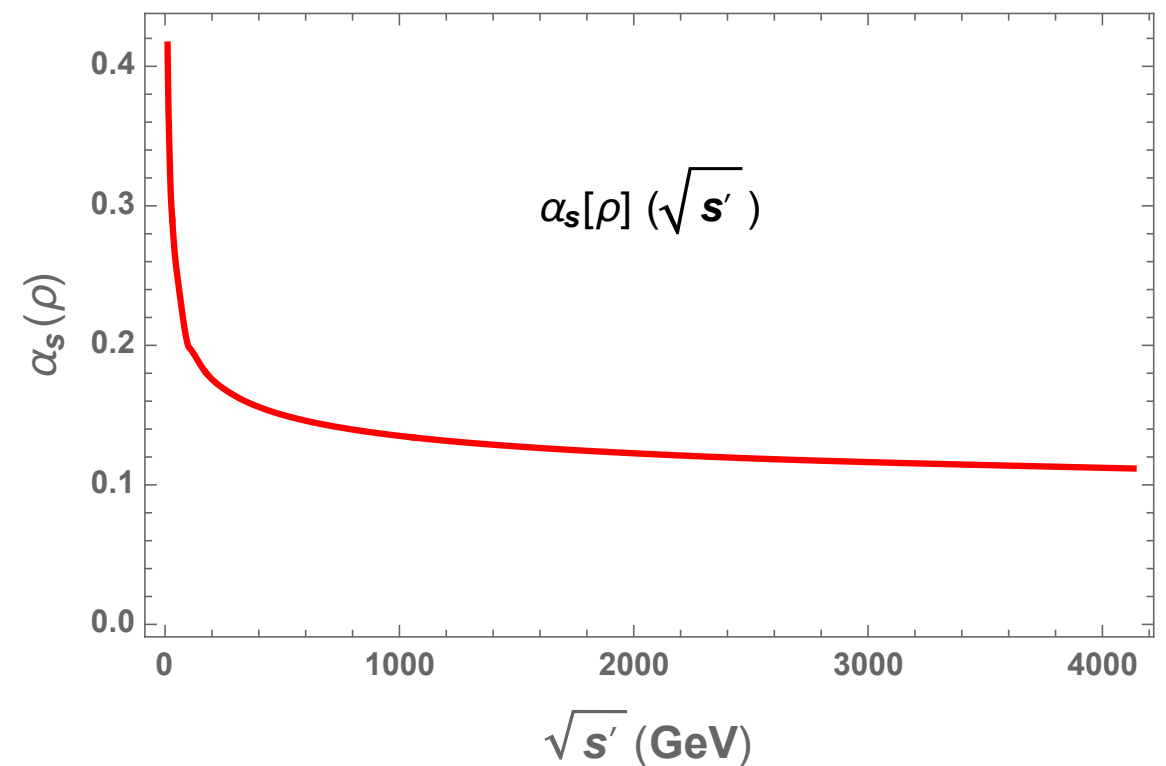
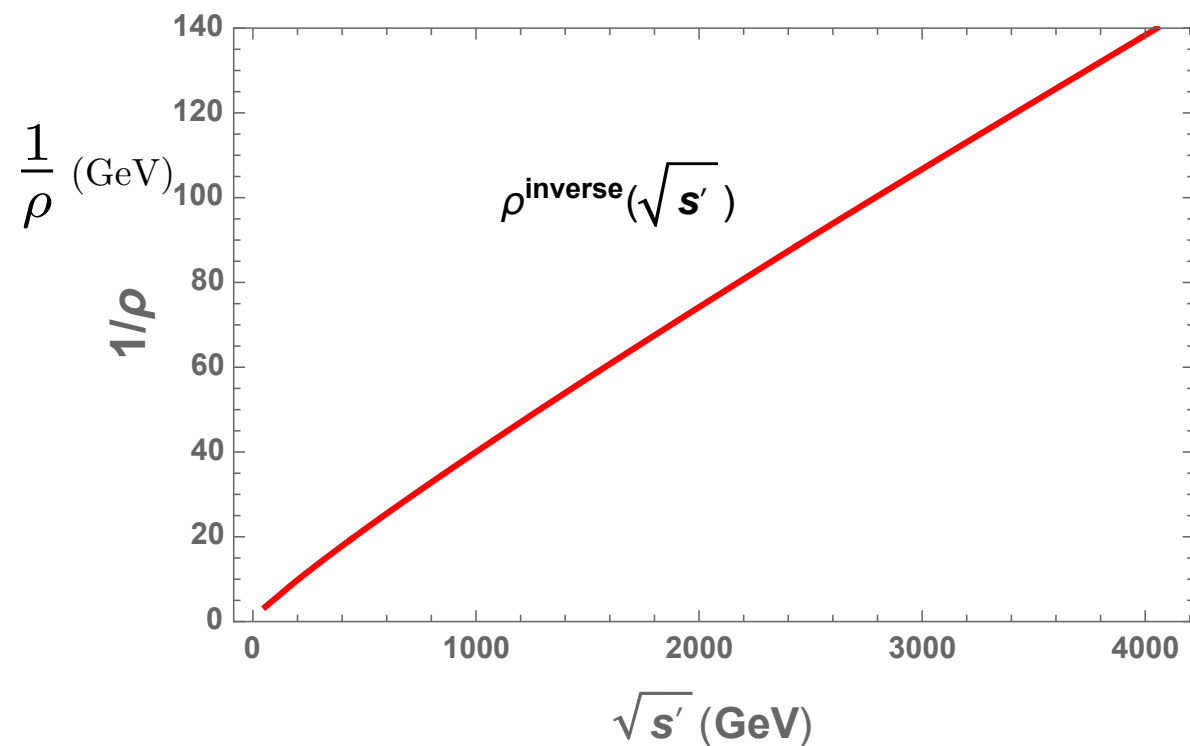
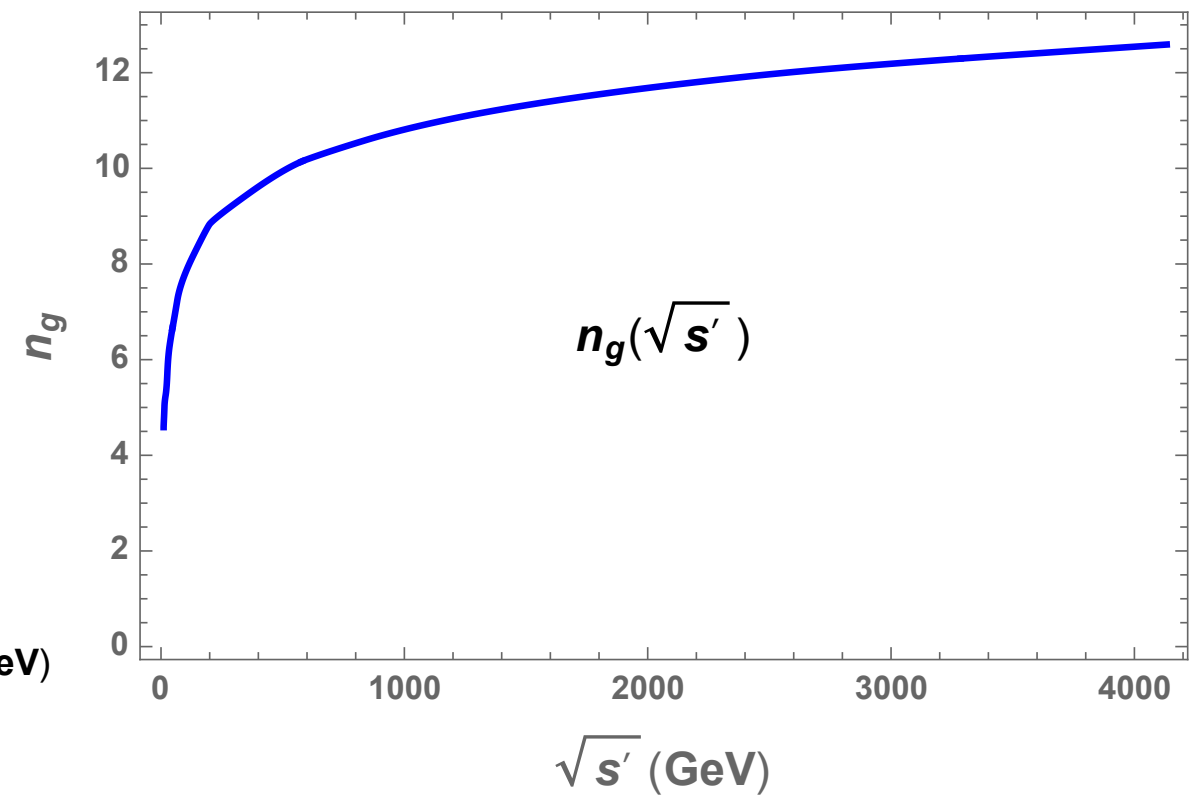
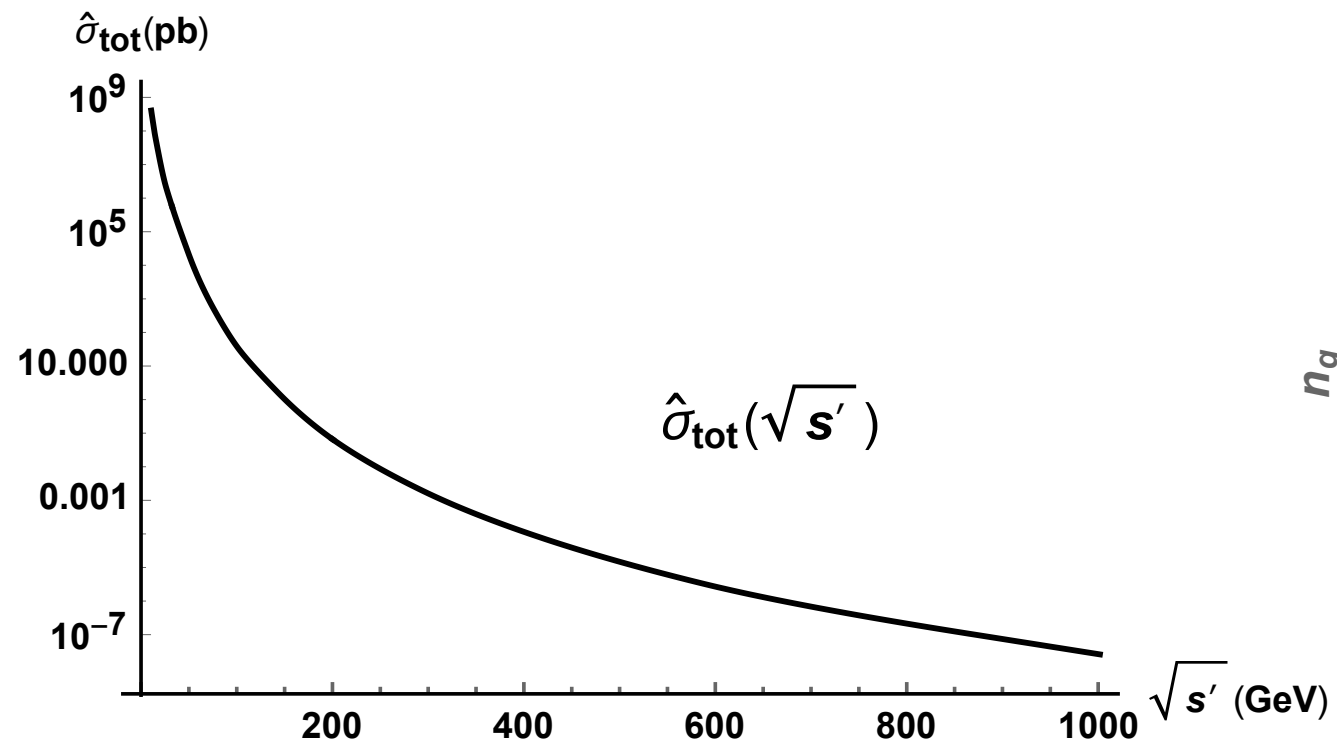
$$\mathcal{F} = \rho \chi \sqrt{s} - \frac{4\pi}{\alpha_s(\rho)} \mathcal{S}(\chi) - \frac{\alpha_s(\rho)}{4\pi} \rho^2 s \log(\sqrt{s} \rho)$$

$$\tilde{\rho} = \frac{\alpha_s(\rho)}{4\pi} \sqrt{s} \rho, \quad \chi = \frac{R}{\rho}$$

2. Carry out all integrations using the steepest descent method evaluating the determinants of quadratic fluctuations around the saddle-point solution
3. Pre-factors are very large — they compete with the semiclassical exponent which is very small!

Results

1st Approach: VVK, Krauss, Schott



2nd more direct approach: VVK, Milne, Spannowsky

compute all (but one) collective coordinate integrals numerically using numerical techniques

introduce dimensionless integration variables,

$$\begin{aligned} r_0 &= R_0 E, & r &= |\vec{R}| E, \\ y &= \rho \bar{\rho} E^2, & x &= \rho / \bar{\rho}, \end{aligned}$$

numerically evaluate (no saddle point approximation needed):

$$\begin{aligned} G(r_0, E) &= \frac{\kappa^2 \pi^4}{2^{17}} \sqrt{\frac{\pi}{3}} \int_0^\infty r^2 dr \int_0^\infty \frac{dx}{x} \int_0^\infty \frac{dy}{y} \left(\frac{4\pi}{\alpha_s} \right)^{21/2} \left(\frac{1}{1 - \mathcal{S}(z)} \right)^{7/2} \\ &\quad \mathcal{K}_{\text{ferm}}(z) \exp \left(-\frac{4\pi}{\alpha_s} \mathcal{S}(z) - \frac{\alpha_s}{4\pi} \frac{x + 1/x}{4} y \log y \right). \end{aligned}$$

and use this to compute the final integral (in the saddle-point approximation to get Im):

$$\hat{\sigma}_{\text{tot}}^{\text{inst}}(E) = \frac{1}{E^2} \text{Im} \int_{-\infty}^{+\infty} dr_0 e^{r_0} G(r_0, E),$$

Results and partonic cross-section

$\sqrt{\hat{s}}$ [GeV]	50	100	150	200	300	400	500
$\langle n_g \rangle$	9.43	11.2	12.22	12.94	13.96	14.68	15.23
$\hat{\sigma}_{\text{tot}}^{\text{inst}}$ [pb]	207.33×10^3	1.29×10^3	53.1	5.21	165.73×10^{-3}	13.65×10^{-3}	1.89×10^{-3}

$$G(r_0, E) = \frac{\kappa^2 \pi^4}{2^{17}} \sqrt{\frac{\pi}{3}} \int_0^\infty r^2 dr \int_0^\infty \frac{dx}{x} \int_0^\infty \frac{dy}{y} \left(\frac{4\pi}{\alpha_s} \right)^{21/2} \left(\frac{1}{1 - \mathcal{S}(z)} \right)^{7/2} \mathcal{K}_{\text{ferm}} \sum_{n_g=0}^{\infty} \frac{1}{n_g!} (U_{\text{int}})^{n_g} \exp \left(-\frac{4\pi}{\alpha_s} - \frac{\alpha_s}{4\pi} \frac{x + 1/x}{4} y \log y \right).$$

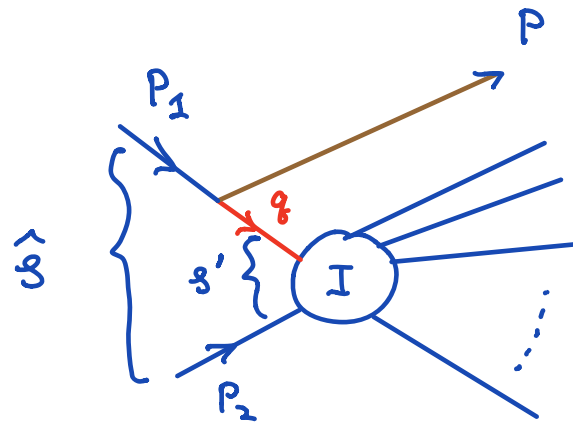
$$\langle n_g \rangle = \langle U_{\text{int}} \rangle$$

hadronic total cross-section

$$\sigma_{pp \rightarrow I}(\hat{s} > \hat{s}_{\min}) = \int_{\hat{s}_{\min}}^{s_{pp}} dx_1 dx_2 f(x_1, Q^2) f(x_2, Q^2) \hat{\sigma}(\hat{s} = x_1 x_2 s_{pp})$$

E_{\min} [GeV]	50	100	150	200	300	400	500
$\sigma_{p\bar{p} \rightarrow I}$ $\sqrt{s_{p\bar{p}}} = 1.96$ TeV	2.62 μb	2.61 nb	29.6 pb	1.59 pb	6.94 fb	105 ab	3.06 ab
$\sigma_{pp \rightarrow I}$ $\sqrt{s_{pp}} = 14$ TeV	58.19 μb	129.70 nb	2.769 nb	270.61 pb	3.04 pb	114.04 fb	8.293 fb
$\sigma_{pp \rightarrow I}$ $\sqrt{s_{pp}} = 30$ TeV	211.0 μb	400.9 nb	9.51 nb	1.02 nb	13.3 pb	559.3 fb	46.3 fb
$\sigma_{pp \rightarrow I}$ $\sqrt{s_{pp}} = 100$ TeV	771.0 μb	2.12 μb	48.3 nb	5.65 nb	88.3 pb	4.42 pb	395.0 fb

If the instanton is recoiled by a *high p_T jet emitted from one of the initial state gluons* \Rightarrow *hadronic cross-section is tiny*



$$Q^2 = -q^2 = \sqrt{\hat{s}} p_T$$

$$s' = (q + p_2)^2 = \hat{s} - 2Q^2$$

A virtual leg

$$\Rightarrow e^{-Q^2} \leftarrow \text{form factor.}$$

\uparrow cuts-off

low-energy range.

Mueller corr.s

cuts-off high-energy range (as before.)

$$\exp(-Q(\rho + \bar{\rho})) = \exp\left(-\frac{Q}{E} \sqrt{y(x + 1/x + 2)}\right)$$

$\sqrt{\hat{s}}$ [GeV]	310	350	375	400	450	500
$\hat{\sigma}_{\text{tot}}^{\text{inst}}$ [pb]	3.42×10^{-23}	1.35×10^{-18}	1.06×10^{-17}	1.13×10^{-16}	9.23×10^{-16}	3.10×10^{-15}

Table 3. The instanton partonic cross-section recoiled against a hard jet with $p_T = 150$ GeV emitted from an initial state and calculated using Eq. (3.7). Results for the cross-section are shown for a range of partonic C.o.M. energies $\sqrt{\hat{s}}$.

$\sqrt{\hat{s}}$ [GeV]	100	150	200	300	400	500
$\hat{\sigma}_{\text{tot}}^{\text{inst}}$ [pb]	1.68×10^{-7}	1.20×10^{-9}	3.24×10^{-11}	1.84×10^{-13}	4.38×10^{-15}	2.38×10^{-16}

Table 4. The cross-section presented for a range of partonic C.o.M. energies $\sqrt{\hat{s}} = E$ where the recoiled p_T is scaled with the energy, $p_T = \sqrt{\hat{s}}/3$.

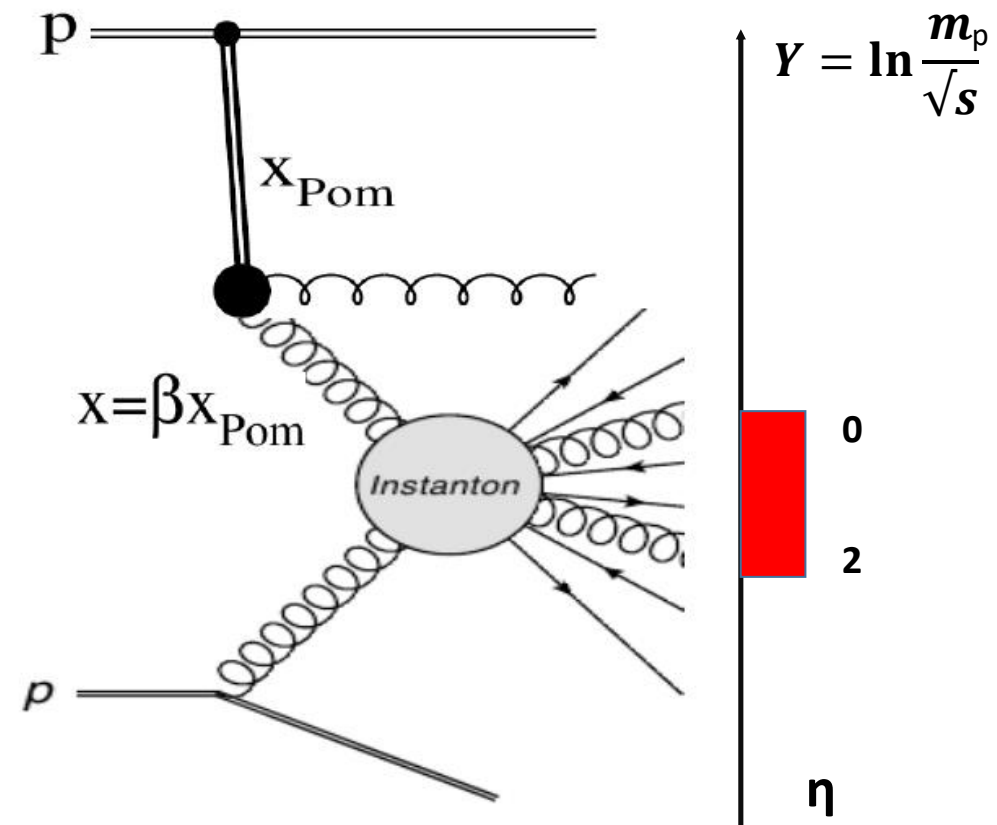
Phenomenology summary (so far)

- QCD instanton cross-sections can be very large at hadron colliders.
- Instanton events are isotropic multi-particle final states. Their event topology is very distinct (see Event shape observables next slide)
- Particles with large p_T emitted from the instanton are rare. Especially hard to produce them at low partonic energies (for obvious kinematic reasons). Do not pass triggers.
- At higher (partonic) energies instanton events can pass triggers but have suppressed cross-sections.
- Alternative approach: consider instanton production in diffractive processes with one or two large rapidity gaps (LRG).

Instanton cross-sections are large, but one needs to be creative in separating instanton signal from large QCD background.

One such strategy is search for QCD instantons in diffractive events at the LHC: QCD background caused by multi-parton interactions can be effectively suppressed by selecting events with large rapidity gaps

$$\sum_i E_{T,i} > 30 \text{ GeV}, N_{ch} > 25$$



use multi-jet cuts

use low luminosity runs to avoid problems with large pile-up

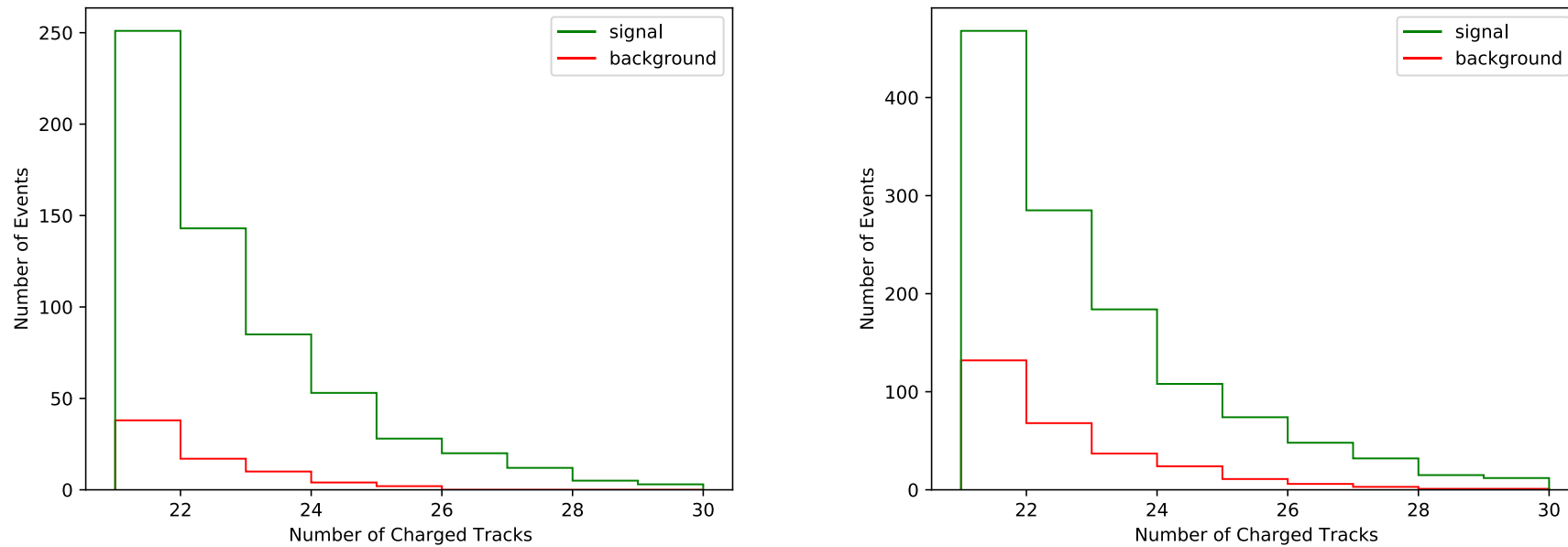


Figure 3: Multiplicity distribution of charged hadrons produced in the events with the instanton (green) in comparison with the expected background (red).

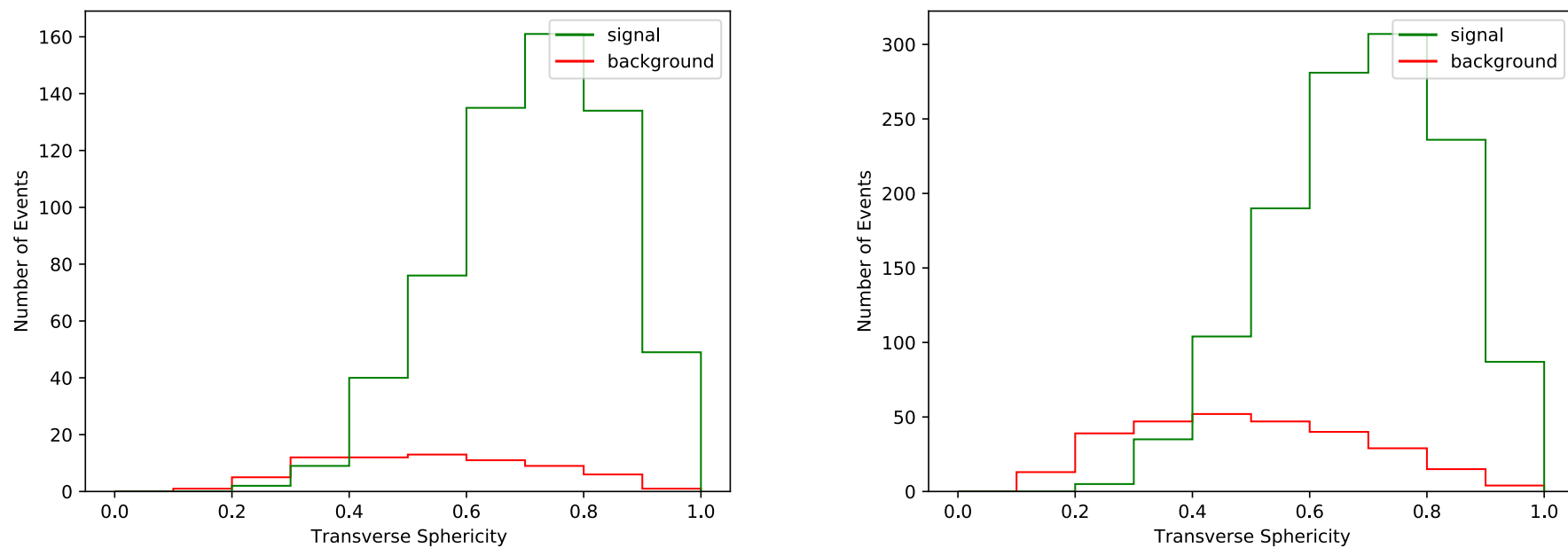
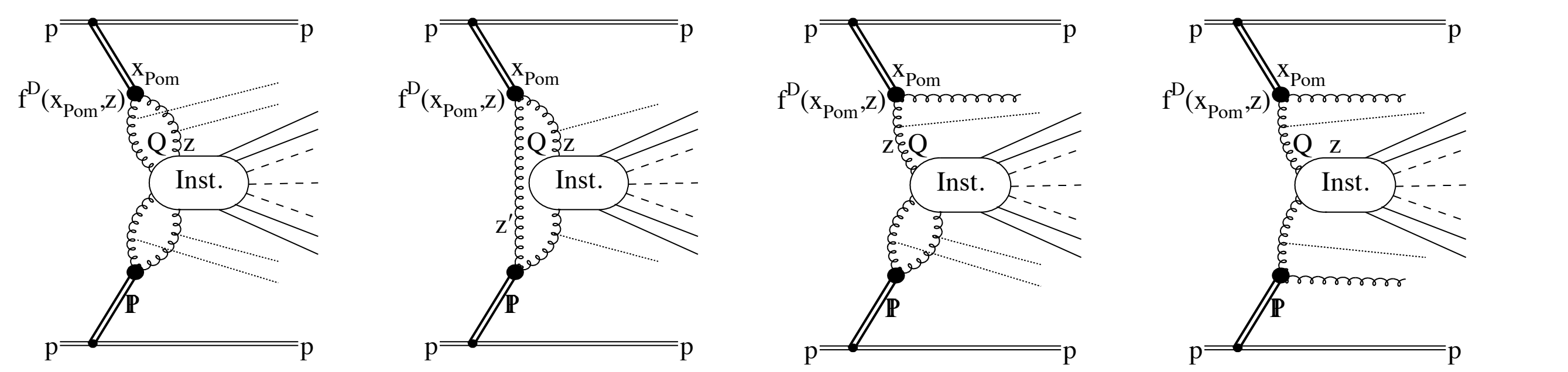


Figure 4: Distribution over the transverse sphericity S_T , Eq. (8), of the charged hadrons produced in the events with the instanton (green) in comparison with the expected background (red).

One can also consider central instanton production in diffractive events with two rapidity gaps:



Latest theoretical results look promising. More detailed phenomenological and ultimately experimental studies are needed and will hopefully follow.

VA Khoze, VVK, Dan Milne, Misha Ryskin: 2111.02159

Extra Slides

Main sources of theoretical uncertainties

- QCD Instanton rates are interesting in the regime where they become large — lower end of partonic energies 20-80 GeV. The weak coupling approximation used in the semiclassical calculation can be problematic. How to address: vary s' minimal partonic energy cutoff. Or even better (when possible) to kill very low s' with cuts.
- What is the role of higher-order corrections to the Mueller's term in the exponent?
- Possible corrections to the instanton-anti-instanton interaction at medium instanton separations in the optical theorem approach.
- Non-factorisation of the determinants in the instanton-anti-instanton background in the optical theorem. (Instanton densities $D(\rho)$ do not factorise at finite $R/\rho \sim 1.5 - 2$.)
- Choice of the RG scale = $1/\rho$. (can vary by a factor of 2 or use other prescriptions to test. In Ref. [1] we checked that)
- A practical point for future progress is to test theory normalisation of predicted QCD instanton rates with data. [The unbiased and un-tuned theory prediction is promising.]

HOW QCD instantons address criticism of EW sphaleron production in high-E collisions:

The sphaleron is a semiclassical configuration with

$$\text{Size}_{\text{sph}} \sim m_W^{-1}, \quad E_{\text{sph}} = \text{few} \times m_W / \alpha_W \simeq 10 \text{ TeV}.$$

It is ‘made out’ of $\sim 1/\alpha_W$ particles (i.e. it decays into $\sim 1/\alpha_W$ W’s, Z’s, H’s).

$$2_{\text{initial hard partons}} \rightarrow \text{Sphaleron} \rightarrow (\sim 1/\alpha_W)_{\text{soft final quanta}}$$

The sphaleron production out of 2 hard partons is unlikely.

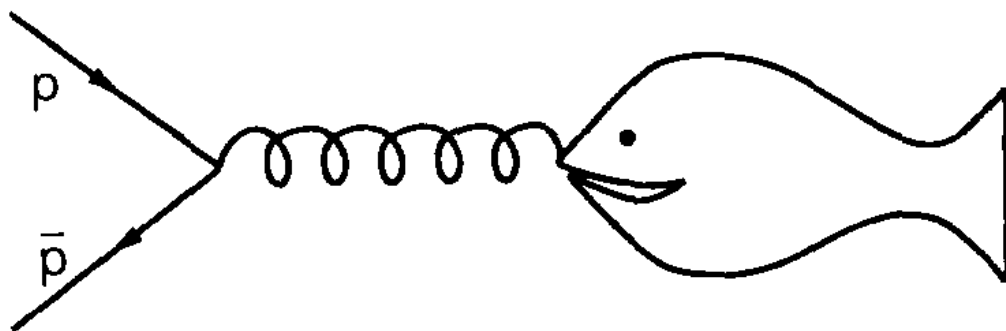


Fig. 3. “You can’t make a fish in a $p\bar{p}$ collider.”

from Mattis PRpts 1991

But in QCD instantons are small
[A ‘small fish’ compared to the EW case]

**This criticism does not apply
to our QCD calculation**